Nuclear Incorporation of Iron during the Eukaryotic Cell Cycle

Ian Robinson[a,b], Yang Yang[c], Fucai Zhang[a,b], Christophe Lynch[a,b] and Yusuf Mohammed[a,b]

[a] Research Complex at Harwell, Rutherford Appleton Laboratory, Didcot, Oxon, OX11 0FA, UK
[b] London Centre for Nanotechnology, University College London, WC1E 6BT, UK
[c] European Synchrotron Radiation Facility, 38043 Grenoble, France

Scanning X-ray fluorescence microscopy has been used to probe the distribution of S, P and Fe within cell nuclei. Nuclei, which may have originated at different phases of the cell cycle, are found to show very different levels of Fe present with a strongly inhomogeneous distribution. P and S signals, presumably from DNA, are high and relatively uniform across all the nuclei; these agree with coherent zoom holography phase contrast images of the same samples. We discuss possible reasons for the Fe incorporation.

1. Introduction

Human cell nuclei are appropriate test samples for the Nanoscale Imaging (NI) branch of the new "NINA" beamline (ID16A) at ESRF, described by Martinez-Criado *et al* (2012). Their sizes are in the range of 10μm, which falls within the field of view of the propagation-based phase contrast imaging capability of ID16A. In addition, high-resolution substructure is expected, at least if the nuclei are close to the metaphase point of the cell cycle when the parent cell is preparing for division. For the fluorescence imaging capabilities of ID16A, known quantities of DNA and (to a lesser extent) proteins are expected to be present in a cell nucleus, which can be used in quantitative chemical analysis and to verify the calibration of the sensitivity.

Nuclei close to metaphase were targeted in this study because of interest in the higher-order structure of the separated chromosomes located within them, but it was also appreciated that this really needs a three-dimensional (3D) imaging capability to segregate them. Our sample preparation methods make use of cell cycle checkpoint inhibitors to synchronize the cells during culture, but this still allows some nuclei to emerge from the preparations at other points of the cell cycle. Careful filtering is used to remove cytoplasm and most of the other cell components (Yusuf *et al*, 2014), so a relatively pure preparation of whole nuclei and individual chromosomes is obtained, many with the nuclear membrane intact. This strictly excludes nuclei in metaphase proper, once the nuclear membrane dissolves, but does include prophase just beforehand, when the 46 chromosomes are fully formed within a nucleus. If the cells were in G1 phase when the samples were prepared, they would contain two double-stranded copies of all the genomic DNA; if they were in G2 phase or the beginning of metaphase (M-phase), there should be four copies; in S phase, there would be somewhere between two and four copies.

The full human genome contains 3.2×10^9 base pairs (bp) per double-strand of DNA, which is divided into the 23 chromosomes. Associated with each base pair are two phosphates, one on each strand. These are by far the largest expected contribution to the P fluorescent X-ray signal, with small additional amounts coming from buffers, the lipids in the cell membranes and any residual RNA or ATP. So a cell nucleus should have a well-defined signal from these 2.6×10^{10} P atoms in its fluorescent images if it is in the second half of the cell cycle (G2 or M phase), or 1.3×10^{10} P atoms in its fluorescent images if it is in the first half of the cell cycle (G1 phase).

Similarly, the S signal would be mostly attributed to Cysteine (Cys) and Methionine (Met) residues in the nuclear proteins. Fortunately, much is known about the make-up of the (mostly structural) chromosomal proteins found in metaphase from the work of Uchiyama *et al* (2005): 71% of the total mass is histones, which are the core proteins around which the DNA is spooled to make nucleosomes. The histones contain many basic Arginine and Lysine groups, which help neutralize the negative charge carried by the DNA. One nucleosome typically occupies 170 base pairs of DNA and, since most of the DNA can be assumed to have condensed into nucleosomes, we can use this to estimate the expected total amount of protein per nucleus. Moreover, the histone sequences are all known, so we can expect there to be 14 S atoms (2xCys and 12xMet) per 170 bp of DNA associated with the histones (Mariño-Ramírez *et al*, 2011). We therefore expect a cell nucleus to have 2.1×10^9 S atoms in its fluorescent images in G2 or M phase and 1.0×10^9 S atoms in G1 phase.

The presence of Fe in the cell nucleus has been discussed repeatedly in the scientific literature. Yagi *et al* (1992) have suggested there may be an evolutionary connection between iron and DNA because of the powerful redox potential of Fe. Fe is an essential element of proteins, often in the form of iron-sulfur (FeS) clusters used in electron transport enzymes (Johnson *et al*, 2005) or in heme complexes in cytochromes (Dawson, 1988). Iron can be toxic to cells via the generation of free radicals (Yagi *et al*, 1992). Since the presence of iron can lead to DNA damage pathways, there may be evolutionary advantage to keeping the DNA in its own nuclear compartment, away from many of the metabolic processes.

Despite the view that Fe-containing enzymes would not be widely used within the nuclear compartment of the cell, there have been recent reports of FeS-containing enzymes directly involved with DNA replication. DNA primase was found to contain an FeS domain (Klinger *et al* 2007, Weiner *et al* 2007) along with DNA helicase (Wu and Brosh, 2012) and DNA repair glycosylases (Wu and Brosh, 2012). A review by Lill *et al* (2006) named five associations of FeS proteins with the cell nucleus: DNA glycosylase (Ntg2), Histone acetyltransferase (Elp3), P-loop ATPase (Nbp35), Iron-only hydrogenase (Nar1) and ABC protein (Rli1). All of theses functions are believed to be associated with DNA replication and repair so should be expressed only during S-phase of the cell cycle and should be absent during other phases.

Ferritin, the Eukaryotic iron storage protein, is not expected to be colocalized with DNA, yet this was reported in a few diverse examples by Thompson *et al* (2002). Nuclear ferritin might be associated with the protection of DNA or conversely with oxidative DNA damage. If nuclear ferritin is present, it might be expected to be associated with the nuclear membrane, rather than mixed in with the DNA-containing chromatin. To address these questions, Fluorescent X-ray imaging of human cell nuclei was undertaken in the work reported here.

2. Methods

2.1 Sample preparation

Nuclei were prepared according to a previously published filtration-based protocol for chromosomes (Yusuf *et al*, 2014) with modifications to preserve the intact nuclei. Human Lymphocyte cells were cultivated in Fetal Bovine Serum (FBS) and treated with Colcemid to arrest them in metaphase. Following extraction, the nuclei were fixed in 0.5% Glutaraldehyde containing 10mM Hepes-KOH and 5mM $MgCl_2$. The samples were pipetted in 5µL drops onto 200nm thick silicon nitride windows and stained with 150µM Syber gold dye. After washing in water, the samples were left to dry in air. They were imaged using a Zeiss AxioZ2 microscope (using "Isis" software) to obtain visible light and optical fluorescence images for reference and correlation with the X-ray results.

For X-ray imaging, several membranes were prepared with the same sample material. The resulting samples were found to contain a large number of intact nuclei, but also chromosome spreads and individual chromosomes from burst nuclei. Some of the membrane-bound samples were stained with platinum blue (Wanner and Formanek, 1995), at 5mM for 30 minutes and washed in water, but no significant differences were found in the phase contrast images and no Pt signal was detected in fluorescence. Results are reported from samples prepared without Pt staining. After the X-ray experiment, the samples were reimages with an Olympus LEXT 4000 confocal microscope to obtain further reference images of the relevant samples.

2.2 X-ray measurements

Samples on membranes were clamped into the sample insertion stubs designed for ID16A. These were load-locked into the UHV sample chamber under vacuum at room temperature by dropping them from a manipulator into the piezo-driven sample stage. The piezo drive system was kept active during this operation so that the contact forces could be monitored in order to prevent overloading the stages.

The ID16A beamline has a multilayer coated Kirkpatrick-Baez (KB) focusing mirror pair located at 185m from an undulator source operating at 17keV (Morawe *et al*, 2015). The KB system, with extreme demagnification designed for a 14x14nm focus, produced a measured focus of 20x30nm with very high flux from the broad bandpass of the multilayer.

For fluorescent imaging experiments, the sample was raster-scanned across the beam at the focus position in 30nm steps. The forward and backward directed fluorescence was detected by a pair of 6-element silicon drift diode detectors with a dwell time of 100ms (CHECK). Spectra were decomposed into pure signals from the P-K, S-K and Fe-L emission lines at 2014, 2308 and 705eV respectively (CHECK) by principle component analysis and calibrated with standard samples of known mass density (DETAILS).

Data for the phase contrast images were obtained by moving the sample downstream of the focus by a range of distances (DETAILS) and recording the projected image on a lens-coupled FReLoN detector with 2048x2048 pixels, giving an effective pixel size of 1.1µm. These data, measured coherently at four different magnifications, were combined using the holotomography method, now called "zoom" tomography, to obtain full-field quantitative phase contrast images of the sample in transmission (Cloetens *et al*, 1999).

3. Results and Discussion

Figure 1 shows an overview optical fluorescence image taken under the excitation conditions for Syber gold dye, which binds specifically to DNA. While the nuclei are clearly well isolated on the membrane, it is clear that not all of them are equally bright. This suggests that either the dye is unable to penetrate the samples uniformly or, more likely, that some nuclei have become depleted in their DNA content. This might have occurred during the washing steps of the sample preparation, or possibly during handling of the samples. We note that the image was taken shortly after sample preparation, before transporting the samples to ESRF, so this does not take into account the effects of the vacuum sample transfer into the ID16A instrument.

Figure 2 shows comparison images of an isolated nucleus by both available X-ray imaging methods: zoom tomography phase contrast and scanning X-ray fluorescence of the P, S and Fe lines. The total signals for the three elements, integrated over the images and calibrated in units of numbers of atoms, are listed in Table 1. The field of view of this image also contains one or two individual chromosomes in a small cluster at the side. This nucleus contains the least quantity of Fe observed, the lowest level of P and the highest S. The distribution of the P- and S- signals overlay well on top of each other and also agree with the distribution of phase shift measured (QUANTITATIVE ANALYSIS OF PHASE VALUES??). The dome-shaped distribution of all three images is roughly what would be expected for a spherical or hemispherical nucleus with a uniform density of chromatin matter within its volume.

The total P signal coming from 3.9×10^9 P atoms is a factor-of-three below the lower estimate of 1.3×10^{10} P atoms, given above, expected for a nucleus in the first half of the cell cycle. This suggests either a calibration error or that some P has been lost

during the sample preparation and insertion into vacuum. We do not attribute this to radiation damage because the signal levels in the images were found to be reproducible upon repeated scanning. On the other hand, the total fluorescent S signal of 4.3×10^9 atoms is substantially higher than the higher estimate above of 2.1×10^9 S atoms in G2 or M phase. Since this appears to be homogeneously distributed within the chromatin filled region of the nucleus, this suggests that the extra signal may be coming from the 29% non-histone proteins, which may have higher relative levels of Cys and Met amino acids (Uchiyama *et al*, 2005).

Corresponding images from three more nuclei, as labelled in Fig 1 and shown in Fig 3, gave the integrated signals listed in Table 1. The trend is similar with an underrepresentation of P and overrepresentation of S. For the S and P signals from 5 nuclei measured, there are factors of 2 variations from one nucleus to another, which might be inherent measurement errors or variations of sample preparation. The highest P signal does just reach the lower estimate for the amount of DNA present in G1 phase, as does the lowest S signal cross over the expected level for G2/M.

Much greater variation was found in both the masses and distributions of the Fe signal, for which a 27x variation was found. Fig 2 shows the nucleus with the smallest level of Fe, while that of Fig 3(a) has the highest level. Unlike S and P, the Fe signals are strongly clustered and often seen to be located at the periphery of the nuclei. It is therefore concluded the most of the Fe signal is coming from the nuclear membrane structures, rather than the central regions, as discussed further below.

We also note that the separated chromosome structure seen at the top of Fig 2 has colocalised P and S signals coming from its distinct arm regions and a separate Fe signal in the centre, which is depleted in P and S. This is appears to be an agglomeration of two chromosomes on the left and right sides and maybe a piece of Fe-rich nuclear membrane in the centre.

4. Conclusions

For the human lymphocyte cell nuclei presented in this study, the distributions of P and S X-ray fluorescence, associated with the DNA-protein complex of chromatin, are found to be relatively uniform and structureless. This could be because the cells are in interphase (G1, S, or G2 of the cell cycle), when the chromatin is decondensed, or it could be because of insufficient resolution to see the individual chromosomes. A certain amount of modulated structure can be distinguished in the P signals of Fig 3(a) and 3(c), which resembles the expected pattern of condensed metaphase chromosomes, even though they are not fully resolved. If so, these nuclei are in prophase, since they still possess their nuclear membrane.

The levels of both P and S are relatively reproducible from nucleus to nucleus, within a factor of 2. The level of P is systematically lower than expected from the number of P atoms contained in the DNA of the human genome. Noting that some

relatively empty (deflated) nuclei were observed in the optical fluorescence image of Fig 1, this may be caused by partial loss of chromosomes during the washing step of sample preparation. It is unfortunate that such losses have taken place as a reliable P level measurement could have been a useful determination of the phase of the cell cycle. Both the levels of S and the S/P ratios are found to be higher than expected from the histone proteins alone, which comprise 71% of the total chromosomal protein. This suggests that the non-histone proteins may be richer in Cys and Met residues.

The Fe concentration, while 3 orders of magnitude lower than P or S, is much more varied among the samples examined, by 27-fold among the integrated signals in Table 1. Fe is not expected to be associated with DNA in general for evolutionary reasons (Yagi *et al*, 1992), yet some exceptions, particularly during DNA replication in S phase, are noted above. Fe is seen to form small bright spots, about 100nm in diameter, in the samples shown in the low-concentration cases in Figs 2 and 3(b). In one case, Fig 3(b), Fe spots are colocalised with S, perhaps suggesting the presence of FeS enzymes; in the other cases, Fig 2, Fe and S are separately localized in spots.

Fe is seen to form shell-like crescent-shaped plaques around the edges of the high-Fe concentration nuclei in Figs 3(a) and 3(c). These are a strong suggestion of Fe being located in the nuclear membrane, rather than the chromatin-filled centres. In most cases the Fe signal can be seen to surround that of the P and S. This may therefore be consistent after all with the evolutionary hypothesis of Yagi *et al* (1992).

As far as we can tell, the zoom tomography measurements did no noticeable damage to the samples, even after multiple and longer exposures were tested. The beam is substantially out of focus here, enlarged to more than the 20x20μm field of view in the closest-distance case. However the raster-scanning fluorescence measurement did cause visible changes to the sample, as recorded in Fig 4. Thinning of the membrane over the entire scanned area can be detected in the confocal height map (grey scale image). Multiple overlapping scanned areas can be observed for the upper nucleus, for which the images appear in Fig 3(b). However, no mass loss between theses scans was detected in the fluorescence signal.

Acknowledgements

This work was supported by a BBSRC Professorial Fellowship BB/H022597/1 "Diamond Professorial Fellowship for imaging chromosomes by coherent X-ray diffraction". Additional support came from an EPSRC grant EP/I022562/1 “Phase modulation technology for X-ray imaging”. We thank ESRF for beamtime and hospitality during the measurements.

References

Cloetens, P., Ludwig, W, Baruchel, J, Van Dyck, D, Van Landuyt, J, Guigay, JP and Schlenker, M (1999), Holotomography: Quantitative phase tomography with micrometer resolution using hard synchrotron radiation x rays, Appl. Phys. Letts. **75** 2912-2914

Dawson, JH (1988) Probing Structure-Function Relations in Heme-Containing Oxygenases and Peroxidases, Science **240** 433-439

Johnson, DC, Dean, DR, Smith, AD and Johnson, MK (2005), Structure, function, and formation of biological iron-sulfur clusters, Ann. Rev. Biochemistry **74** 247-281

Klinge, S., Hirst, J., Maman JD, Krude T. and Pellegrini, L. (2007), Iron-sulfur domain of the eukaryotic primase is essential for RNA primer synthesis, Nature Structural & Molecular Biology **14** 875

Lill, R., Dutkiewicz, R., Elsässer, H-P, Hausmann, A. Netz, DJA, Pierik, AJ, Stehling, O., Urzica, E. and Mühlenhoff, U., (2006), Mechanisms of iron–sulfur protein maturation in mitochondria, cytosol and nucleus of eukaryotes, Biochimica et Biophysica Acta **1763** 652

Mariño-Ramírez, L., Levine, K.M., Morales, M., Zhang, S., Moreland, R.T., Baxevanis, A.D., and Landsman, D. (2011) The Histone Database: an integrated resource for histones and histone fold-containing proteins. Database Vol.2011: article ID bar048, doi:10.1093/database/bar048.

Martinez-Criado, G, Tucoulou, R, Cloetens, P, Bleuet, P, Bohic, S, Cauzid, J, Kieffer, I, Kosior, E, Laboure, S, Petitgirard, S, Rack, A, Sans, JA, Segura-Ruiz, J, Suhonen, H, Susini, J. and Villanova, J (2012), Status of the hard X-ray microprobe beamline ID22 of the European Synchrotron Radiation Facility, Journal of Synchrotron Radiation **19** 10-18

Morawe, C, Barrett, R, Cloetens, P, Lantelme, B, Peffen, JC, Vivo, A (2015), Graded multilayers for figured Kirkpatrick-Baez mirrors on the new ESRF end station ID16A, Advances in X-Ray/EUV Optics and Components X, Proceedings of SPIE **9588** 958803-1

Thompson, KJ, Fried, MG, Ye, Z., Boyer P. and Connor, JR, (2002), Regulation, mechanisms and proposed function of ferritin translocation to cell nuclei, Journal of Cell Science **115** 2165

Wanner, G; Formanek, H (1995), Imaging of DNA in Human and Plant Chromosomes by High-Resolution Scanning Electron-Microscopy, Chromosome Research **3** 368-374

Weiner, B.E., Huang H., Dattilo, BM, Nilge MJ, Fanning E. and Chazin, W. J. (2007), An Iron-Sulfur Cluster in the C-terminal Domain of the p58 Subunit of Human DNA Primase, J. Biological Chemistry **282** 33444

Wu Y. and Brosh, R.M. (2012), DNA helicase and helicase–nuclease enzymes with a conserved iron–sulfur cluster, Nucleic Acids Research **40** 4247

Yagi, K., Ishida, N., Komura, S., Ohishi, N., Kusai, M. and Kohno, M, (1992), Generation of hydroxyl radical from linoleic acid hydroperoxide in the presence of epinephrine and iron, Biochem. Biophys. Res. Commun. **183** 945–951

Yusuf, M, N. Parmar, G. K. Bhella and I. K. Robinson (2014), A simple filtration technique for obtaining purified human chromosomes in suspension, BioTechniques **56** 257-261

Figures and Tables

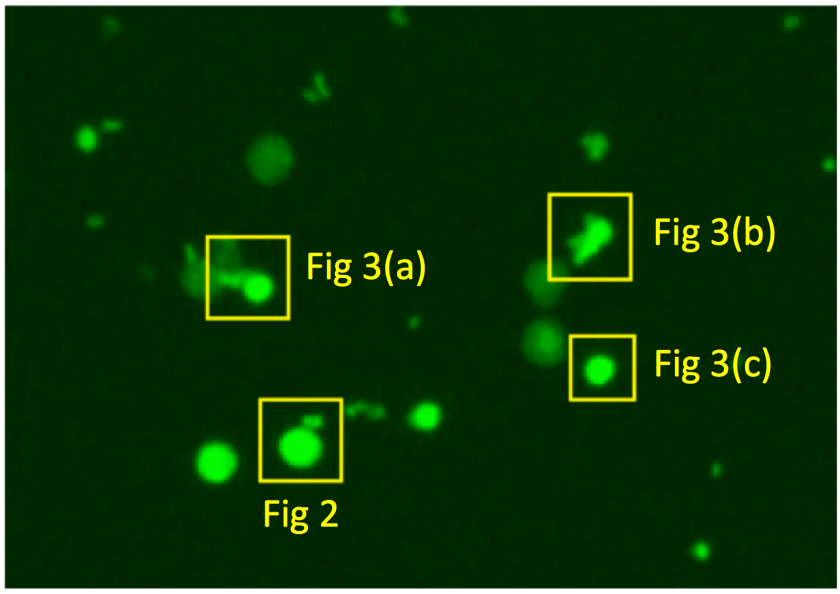

Figure 1. Low magnification optical fluorescence image taken under the excitation conditions for Syber gold dye using a Zeiss AxioZ2 microscope. Boxes and labels indicate the nuclei that are analysed further in this work.

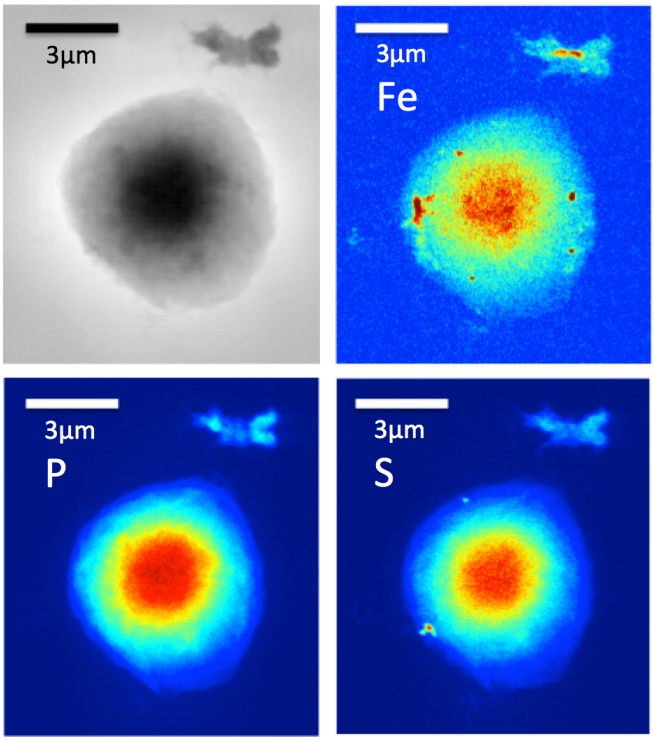

Figure 2. X-ray images of the nucleus outlined in Fig 1, with a group of individual chromosomes on the upper side. Top left: zoom-tomography phase contrast image. Other panels: elemental distributions from raster-scanned fluorescence mapping.

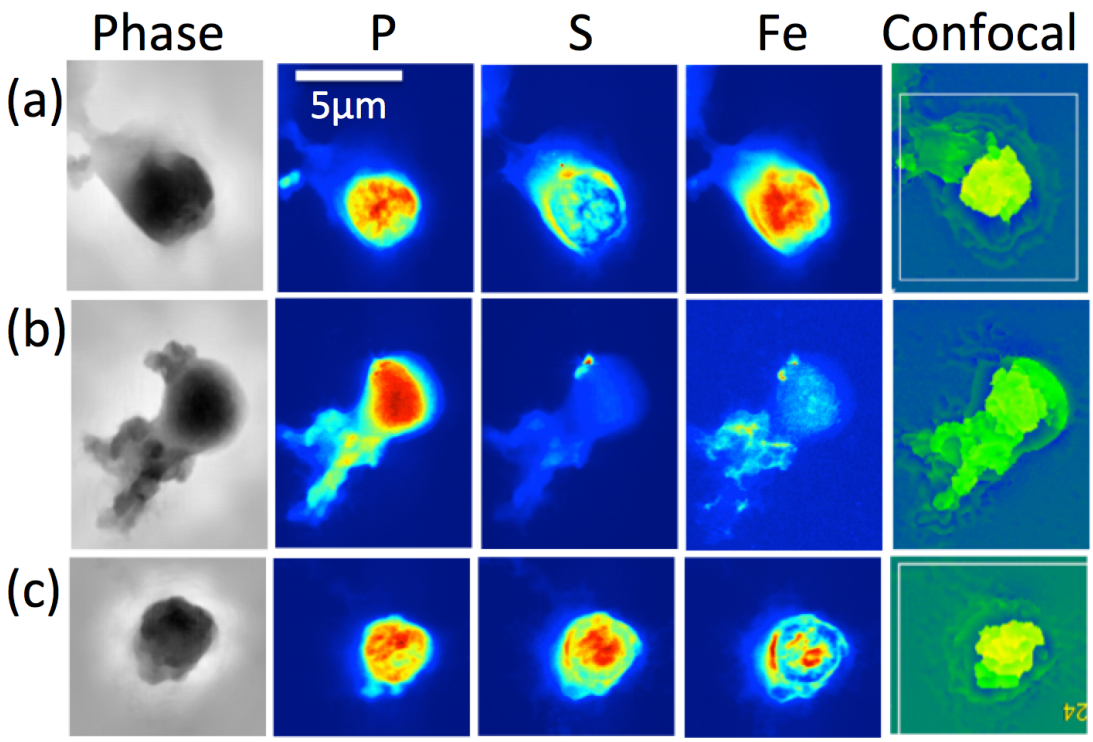

Figure 3. X-ray images of three more nuclei outlined in Fig 1. Left column: zoom-tomography phase contrast image. Centre columns: elemental distributions from raster-scanned fluorescence mapping, scaled to the maximum pixel value. Right: optical confocal height map, measured after the X-ray experiment. The scale bar applies to all panels.

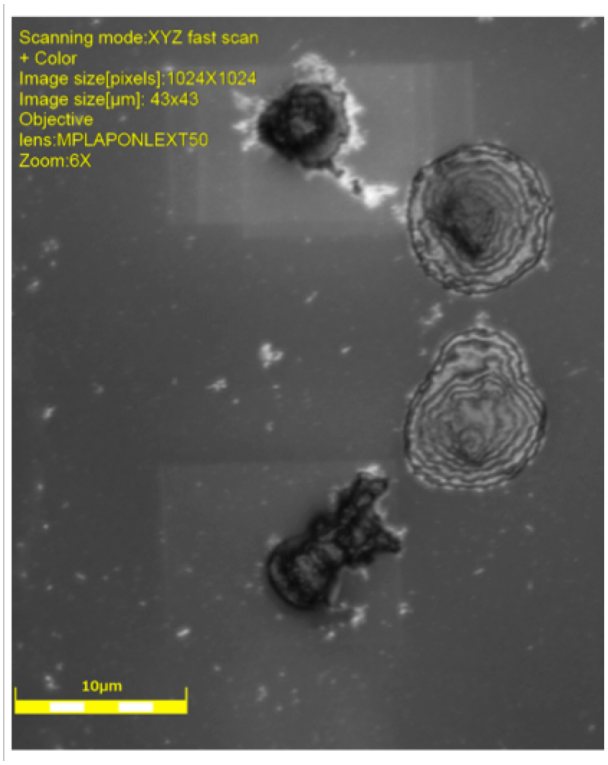

Figure 4. Grey-scale confocal image measured with a 50x lens on an Olympus LEXT 4000 microscope after the X-ray experiment. Nuclei 3(b) and 3(c) can be seen, along with a clear modification to the membrane in the region where the fluorescence mapping had taken place.

Sample	P count	S count	Fe count
Fig 2	3.9×10^{9}	4.3×10^{9}	2.8×10^{6}
Fig 3(a)	9.3×10^{9}	2.6×10^{9}	7.6×10^{7}
Fig 3(b)	6.1×10^{9}	1.5×10^{9}	5.6×10^{6}
Fig 3(c)	7.1×10^{9}	1.8×10^{9}	5.0×10^{7}
Nucleus7	12.8×10^{9}	1.4×10^{9}	1.1×10^{7}
Average	7.8×10^{9}	2.3×10^{9}	
G1 phase	13×10^{9}	1.0×10^{9}	
G2 or M phase	26×10^{9}	2.1×10^{9}	

Table 1. Calibrated X-ray fluorescent signals, integrated over the five most reliable raster scans of human cell nuclei. Derived masses have been converted into numbers of atoms found within the nuclear regions of the samples measured at ID16A. The last two rows give the counts expected for different phases of the cell cycle, as discussed in the text.